

Article

Effects of Clay Minerals and External Pressures on Imbibition in Shales

Li Lu ^{1,2,3} , Jianting Li ⁴, Xuhui Zhang ^{3,4} , Yingjun Li ^{1,*} and Fujian Ma ⁵

¹ State Key Laboratory for Geomechanics and Deep Underground Engineering, China University of Mining and Technology (Beijing), Beijing 100083, China; bqt1700620003@student.cumtb.edu.cn

² Institute of Mechanics, Chinese Academy of Sciences, Beijing 100049, China

³ School of Engineering Science, University of Chinese Academy of Sciences, Beijing 100049, China; zhangxuhui@imech.ac.cn

⁴ Petrochina Changqing Oilfield Company, Xi'an 710016, China; ljt_cq@petrochina.com.cn

⁵ Schlumberger, Beijing 100016, China; fma2@slb.com

* Correspondence: lyj@aphy.iphy.ac.cn

Abstract: Imbibition is an important mechanism of recovery during waterflooding and low flow-back during fracking in shale reservoirs. Experiments were carried out to study the development of imbibition in shale samples. The effects of clay minerals, especially the illite and IS, were mainly investigated and discussed. The imbibition under different pressures was conducted and compared. The influence of clay minerals on imbibition in shale is significant and complex. It is shown that the low content of illite and IS and small capillary force lead to small imbibition mass and speed. Formation of new micro fractures due to the swelling of clay minerals can cause the permeability to increase and the imbibition to be speeded up. The pore structure, the content of IS, and the capillary force affect the imbibition process significantly. The external pressure obviously affects the imbibition speed and the final imbibition mass. The content of clay minerals is more important to the formation of new micro fractures than the external pressure. There is a peak in the curve of displacement efficiency versus the content of either clay minerals or illite and IS. The effect of illite and IS more remarkable.

Keywords: imbibition; shale; clay minerals or illite; IS; NMR



Citation: Lu, L.; Li, J.; Zhang, X.; Li, Y.; Ma, F. Effects of Clay Minerals and External Pressures on Imbibition in Shales. *Energies* **2021**, *14*, 7528. <https://doi.org/10.3390/en14227528>

Academic Editors: Riyaz Kharrat and Kun Sang Lee

Received: 9 September 2021

Accepted: 22 October 2021

Published: 11 November 2021

Publisher's Note: MDPI stays neutral with regard to jurisdictional claims in published maps and institutional affiliations.



Copyright: © 2021 by the authors. Licensee MDPI, Basel, Switzerland. This article is an open access article distributed under the terms and conditions of the Creative Commons Attribution (CC BY) license (<https://creativecommons.org/licenses/by/4.0/>).

1. Introduction

Imbibition is an important recovery mechanism during waterflooding in tight fractured reservoirs. Hydraulic fracturing is a necessary means to effectively exploit shale oil/gas reservoirs [1,2]. In practice, high production rates usually accompany large amounts of hydraulic liquid retention, which can cause the trapping of aqueous phase. However, this can be auto-relieved after shut-in for a certain period. Meanwhile the hydrocarbon recovery is improved. Imbibition is thought to be the main reason [3–5]. Such imbibition may be spontaneous or forced. The main difference between the two mechanisms for imbibition is whether there is acted external pressure besides the capillary force. In a spontaneous imbibition the wetting fluid moves into the pores to displace the non-wetting fluid under capillary force. In forced imbibition the wetting fluid is pushed into pores under external force and the capillary working together.

Previous studies show that the imbibition is closely related with the structure of matrix and fracture, fluid properties such as interfacial tension and wettability, mineral, etc. [6–8]. Large permeability, good pore structure and formation of fractures tend to indicate strong imbibition. The dissolved organic carbon (TOC) weakens the imbibition because of its low permeability and complex pore structure. The clay minerals, especially the illite/smectite formation (IS), swell once they absorb water, which can on the one hand lead the formation of new micro fractures, and on the other hand presses the neighboring pores and narrows

down the pore diameters. Therefore, the effects of clay minerals on the imbibition are complicated. The formation of new micro fractures enhances the imbibition while the shrinkage of pore scales weakens the imbibition because of the decrease of permeability. The final effects are determined by the competition of the two factors [9]. Meng et al. [10] found that the peak of T_2 spectral, measured by using nuclear magnetic resonance (NMR), moves clearly towards the right (large value) during imbibition. The corresponding permeability decreases first and then increases [11,12], which indicates firstly the shrinkage of pore scales and subsequently formation of new micro fractures.

The intergranular space of illite is about 0.34 nm. The diameter of a water molecule is 0.278 nm. So water molecules can totally enter into the intergranular space of illite during imbibition because of the strong absorption and their small diameter [13].

During imbibition, liquid migration from large pores and cracks into small pores can cause an increase in permeability. The large pores and cracks contribute more to permeability than the small pores. The induced cracks, due to clay minerals swelling, play an important role in the relief of trapping in the aqueous phase [14]. Complex physical and chemical interaction between shale and water can change the micro#-structure and induce micro fractures, which leads to the weakening of shale [15,16], e.g., the damage of cement among grains, increase of secondary pores, and micro fractures due to absorption of water by clay [17–19].

Li et al. [20] showed that the presence of clay minerals affects water distribution in shale, which in turn changes the methane adsorption capacity. Zhang et al. [21] showed that the swelling of the clay minerals may be beneficial to oil production. The pores are gradually compressed along with the swelling of clay minerals to increase the oil recovery. They considered that the compaction of pore space due to the swelling of clay minerals during shut-in may be an important mechanism for enhancing oil recovery by imbibition. Yang et al. [4] studied the effects of clay minerals on spontaneous imbibition of shale. The results show that the water volume involved in imbibition in a reservoir with high clay content is generally several times the pore volume. Therefore, the effects of clay minerals on spontaneous imbibition cannot be neglected when considering the oil recovery potential.

Makhanov et al. [9] and Yang et al. [22] showed that the content of clay minerals has positive effects on the oil recovery during spontaneous imbibition. The main reason is that the clay minerals are easy to swell, which results in the deformation of pore structure. Meanwhile, the clay minerals can change the sorption capacity of shale. Plagioclase, kaolinite and quartz have positive impact on the salinity-induced oil removal.

In 1962, Mattax and Kyte [23] presented a model to describe the relation between character time and imbibition length (generally named the M-K model). Kazemi [24] modified the M-K model by considering the factor of pore shape. Ma [25] presented a modified model based on the analysis of the amount of experiment data under different conditions of strong water hydrophilic rock. These studies present the theoretical principles for imbibition in tight rock. However, the previous studies consider only limited factors. Some factors, such as clay minerals, coupling effects of pores and fractures, connectivity, etc., play an important role in imbibition and should be considered in any theoretical model. Before that, the affecting mechanism should be clarified, and quantitative analysis is also very important. Certainly, experimental study is an effective and reliable method.

The aim of this paper is to clarify the characteristics of imbibition in shale containing clay minerals. Experiments were carried out to study the development of imbibition mass and the T_2 spectral with time. The effects of clay minerals, especially illite and IS, were investigated and discussed. The imbibition under different pressures was studied and compared.

2. Materials Preparation and Experimental Methods

2.1. The Physical Properties of Samples

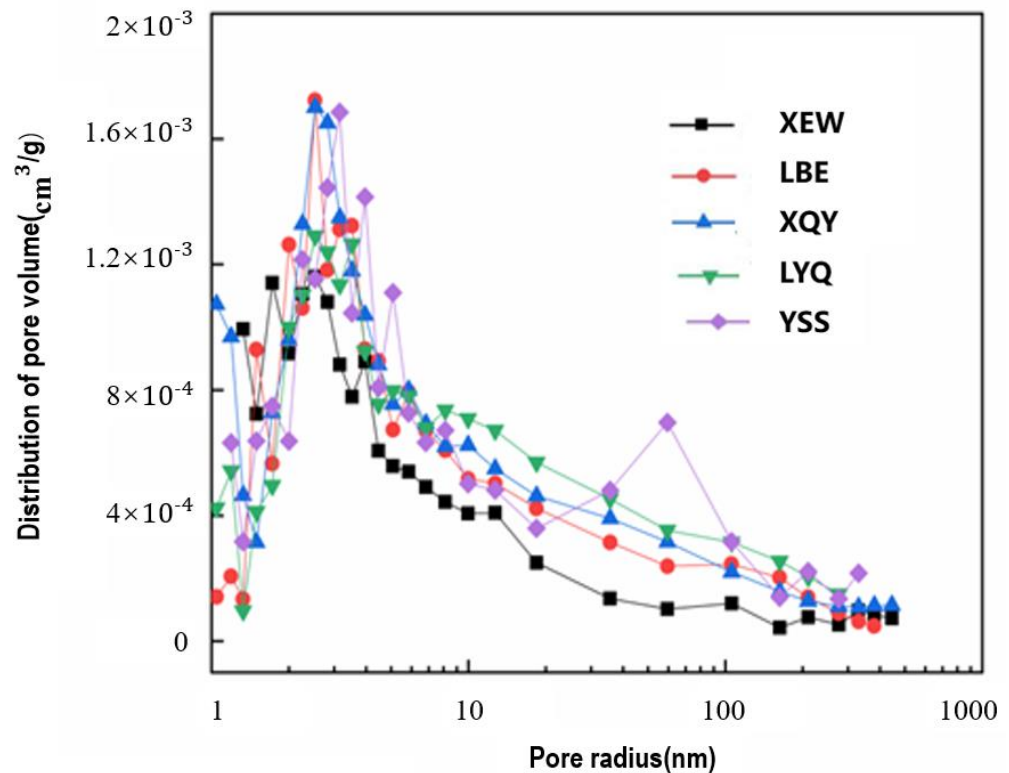
The samples of shale rock were collected from formations of the Ordos Basin. The samples were cored from different wells. A small section of each core was cut before

the imbibition experiments, so that it could be cut into smaller samples for the mercury intrusion test, nitrogen adsorption test, and mineral tests. These measured data can be used to describe the cores.

The sample was first cleaned and crushed, then the powder was dipped in distilled water and oscillated by ultrasonic wave to speed the separation of clay from the particles. The grains with scale less than 2 μm was extracted, dried and weighted. The content of clay is determined by computing the mass ratio of the clay and the total mass. The clay minerals were measured by an X-ray diffraction (XRD) apparatus (MXP21VAHF, made in Japan) at the University of Science and Technology Beijing.

The density was in the range of 2580–2650 kg/m^3 . The samples were all obtained from the low permeable reservoir and the permeabilities were from 1.1×10^{-3} to 0.322 mD. The permeability of sample XEW was the largest and that of sample LBE the smallest. The clay mineral was rich in samples, ranging from 14.4% to 37.9%. The contents of clay minerals were clearly different among samples. The content is only 14.4% in the sample of LYQ while it is 37.9% in XBL. Because of the strong absorption of water, IS has significant effects on imbibition. The contents of IS are in the range of 6.615% (XEW)–21.982% (XBL). LBE has the strongest capillary because of the smallest porosity. The scale of each samples used in experiments is length \times diameter = $5.0 \times 2.5 \text{ cm}^2$.

The pore radii of the samples were measured by combining N_2 absorption (for the pore radii $< 50 \text{ nm}$) and Mercury intrusion (for the radii $> 50 \text{ nm}$). It is shown from Figure 1 that the pore radii are mainly in the range of 50–500 nm and the fractures are obviously developed in samples XQY and LBE. There are two peaks in the distribution curve of pore radius. One is near 3 nm and the other is around 100 nm. During imbibition, micro fractures form in the samples LYQ, LBE and XBL. The other physical parameters are shown in Table 1.



(a)

Figure 1. Cont.

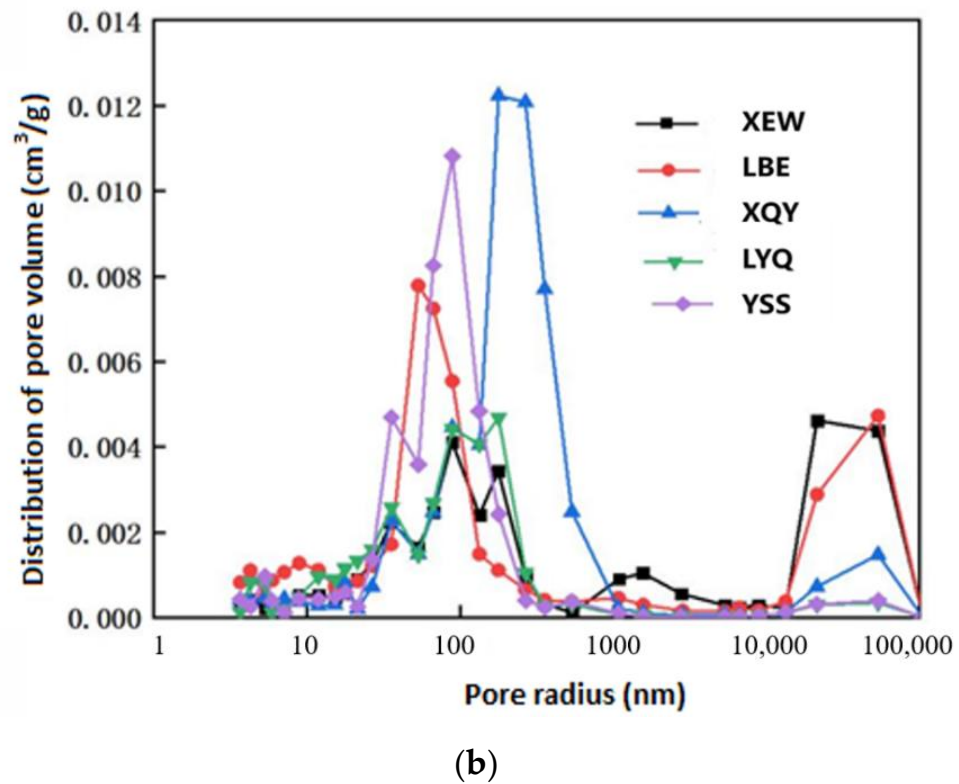


Figure 1. The distribution of pore radius of all samples. (a) Measured by N₂ absorption; (b) Measured by Mercury intrusion.

Table 1. The physical parameters of samples.

No. of Wells	ρ (g/cm ³)	S_w (%)	k (mD)	φ (%)	S_q (%)	S_c (%)	S_{im} (%)	P_{cm} (MPa)	F_n	E_i (%)	H_p (%)
LYQ	2.65	0.4	0.042	5.8	58.4	14.4	8.064	9	✓	44.09	38.69
LBE	2.58	0.5	0.0011	2.7	41.9	30.5	21.35	50	✓	41.89	21.25
XQY	2.58	0.5	0.322	8.2	17.6	20.3	11.165	3			
XBL	2.64	1	0.033	5.4	36	37.9	21.982		✓	9.85	9.96
XEW	2.63	0.6	0.046	6.1	50.2	18.9	6.615	7	×	18.85	20.51
YSS	2.65	1	0.042	7.6	41.7	22.4	11.2	8	×	23.98	24.6

Note: ρ , density; S_w , initial water saturation; k , permeability; φ , porosity; S_q , content of quartz; S_c , content of clay minerals; S_{im} , the contents of IS; P_{cm} , Median of the capillary force; F_n , if there are new micro fractures forming; E_i , displacement efficiency of imbibition; H_p , displacement efficiency of huff and puff development.

2.2. Equipment

Figure 2 shows the apparatus for the imbibition experiments. The sample was totally emerged into heavy water (D₂O) with all boundaries opening in a piston tank and the mass was measured by a digital balance (minimum reading of 1×10^{-5} g) at set intervals. The piston tank is connected to a manual pressurizing pump, and the applied pressure is monitored by a pressure gauge. Shown in Figure 2c is the appearance and connection of the equipment. The equipment can apply a pressure of up to 45 MPa to the liquid in the piston tank.

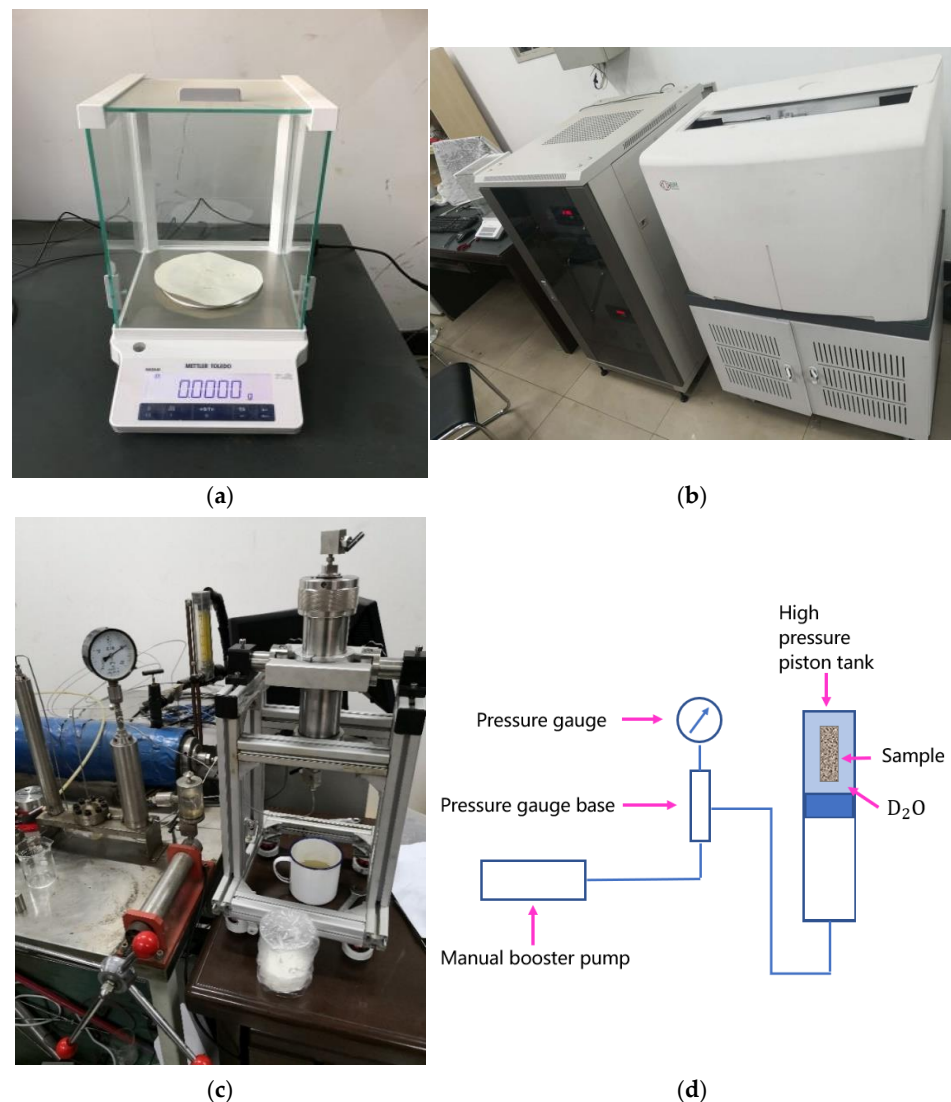


Figure 2. The apparatus used in the experiments. (a) Imbibition setup; (b) Photo of NMR; (c) Manual pressure device; (d) Schematic diagram of manual pressure device.

NMR was used to trace the development of displacement during imbibition by using T_2 (crosswise relaxation time) (Figure 2b). The longer the T_2 relaxation time, the larger the pore scale filled with fluid containing H^+ . Therefore, from T_2 spectra the migration of water in different pores and fractures can be observed clearly, which can help us to trace the advance F of the displacement front during imbibition, the formation of new micro fractures and the imbibition speed in different pores [26]. The invaded heavy water or the displaced oil is equal to the decrease of the surrounding area by T_2 spectra and the horizontal coordinate.

The NMR produced by Shanghai Niumag Corporation (Figure 2) was adopted. This can provide a magnetic field intensity of 0.5 T. To assure the accuracy of the measurement, the waiting time > 8000 ms was adopted. Echo numbers (NECH), signal superposition times (SCANS), were adopted as 2048 and 64, respectively. The echo time interval (TE) was set as 0.3 ms.

2.3. Experimental Procedure

The experimental procedure refers to the experiments done by Yang et al. [4]. Oil-saturated samples were immersed in heavy water and then the oil was displaced due to imbibition. The distribution of the retained oil with time can be traced by the changes of

T₂, because the heavy water cannot induce NMR signals. Before imbibition, all samples were dried till the weight did not change anymore in a drying oven at 105 °C. Then the sample was taken out and placed in a vacuum kettle to evacuate the saturated oil. After the core was fully saturated with oil, it was taken out, and the spontaneous imbibition and the pressure imbibition experiment, respectively, were performed. During the experiment, NMR and precision electronic balances were used to measure the T₂ spectrum and the change of mass. The steps in the experiment are as follows:

1. Spontaneous imbibition experiment under 1 atm:
 - a. Put the sample in the drying oven, set the temperature to 105°, and take it out until the sample is dried to a constant weight (about 24–48 h).
 - b. Put the dried sample in a vacuum kettle to vacuum and to saturate it with oil until the weight of the sample is constant (about 72 h).
 - c. Take out the saturated sample and measure the diameter, length and mass, then scan it by NMR to obtain the T₂ spectrum.
 - d. The sample saturated with oil is completely immersed in the heavy water in a beaker. After soaking for a period of time, remove the sample from the heavy water, and absorb the heavy water on the surface of the sample with absorbent paper, then measure the mass of the sample and scan by NMR to obtain the T₂ spectrum. After measurement, the sample was immersed in heavy water again.
 - e. Repeat step (d); the sample soaking time between two measurements is shorter in the early stage and longer in the later stage.
2. Pressure imbibition experiment:
 - a. Put the sample in the drying box, set the temperature to 105°, and take it out until the sample is dried to a constant weight (about 24 h–48 h).
 - b. Put the dried sample in a vacuum kettle and then immerse it in the oil until the sample has a constant weight (about 72 h).
 - c. Take out the sample saturated with oil, measure the diameter, length and mass of the sample, and scan the T₂ spectrum.
 - d. After the pressurizing device is connected, the sample saturated with oil is completely immersed in the heavy water in the piston tank, the piston tank is sealed, and the pressure is increased to 10 MPa. After a period of time, release the pressure and open the piston tank, take out the sample, and absorb the heavy water on the surface of the sample with absorbent paper, then measure the mass of the sample and scan the T₂ spectrum. After measurement, the sample is immersed in heavy water again.
 - e. Repeat step (d); the sample soaking time between two measurements is shorter in the early stage and longer in the later because the imbibition becomes increasingly slower with time.

3. Results and Analysis

3.1. Spontaneous Imbibition under 1 Atm

The results of imbibition mass with time under 1 atm are shown in Figure 3. The imbibition speeds and the total mass of the samples YSS and XEW are the smallest. The relatively high initial water saturation and low content of illite and IS indicate the poor pore structure and connection, so the imbibition develops slowly, though the permeability is not low. The imbibition mass of the sample LBE is the largest. The imbibition speed of the sample LYQ is the largest. The contents of illite and IS in the samples YSS and XEW are relatively low. Meanwhile the median values of capillary forces are also small. These two reasons cause the imbibition mass and speed to be the smallest. The median value of capillary force of the sample LBE (50 MPa) is the largest in all the samples, which is why the imbibition speed is the largest, except for the first period.

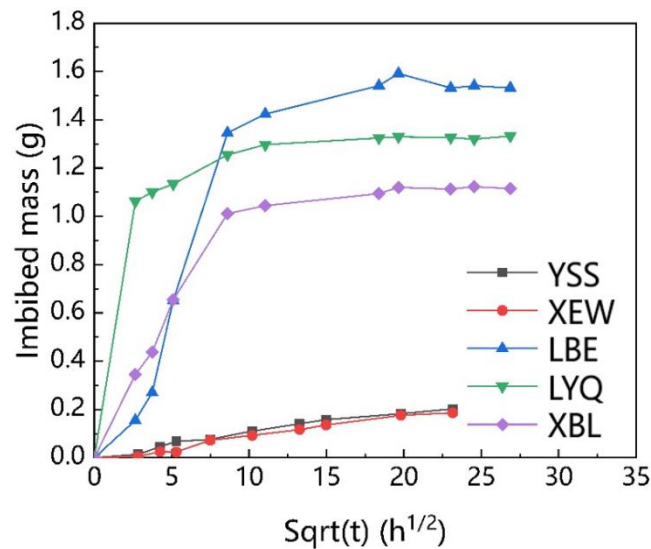


Figure 3. The development of imbibition mass with time.

From the T_2 spectral, it can be seen that the imbibition of the sample YSS develops fast in the small pores. Some of the oil in the small pores is displaced into the large pores. During imbibition, there are no micro fractures formed (Figure 4). The reason may be the relatively large porosity, 7.6%, as the swelling is not enough to damage the shale structure, though the content of IS (11.2%) is not low. Compared with YSS and XEW, the heavy water in the sample LYQ is distributed in a narrow range of porosity. There is no obvious displacement of oil from small pores into large pores at the first stage until the occurrence of new fractures due to the swelling of clay minerals (Figure 5a). From Figure 5a, it can also be seen that there are large pores or fractures forming at $T_2 = 600\text{--}1000$. After the experiment, an obvious small fracture can be observed on the surface of the sample (Figure 5b). Because of the low content of IS, 8.064%, and the formation of new micro fractures, the displacement efficiency is higher than that of the other samples.

The results indicate that low content of illite and IS and small capillary force generally means slow imbibition. The pore structure, the content of illite and IS, and the capillary significantly affect the imbibition process.

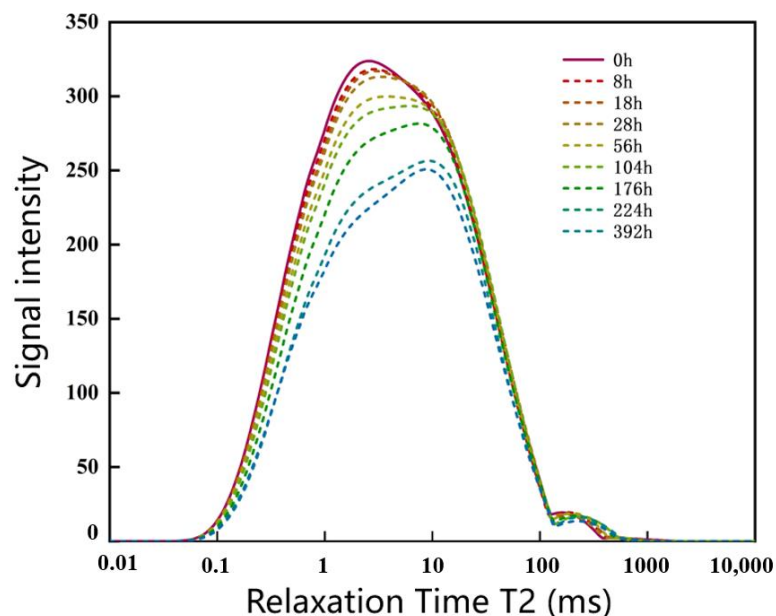
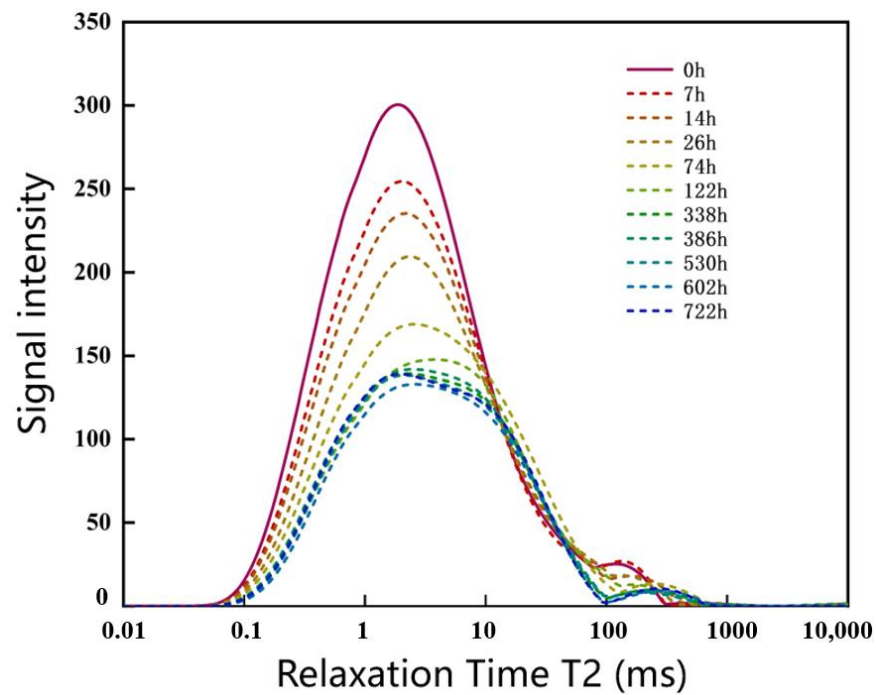


Figure 4. Development of T_2 of sample YSS at 1 atm.



(a)



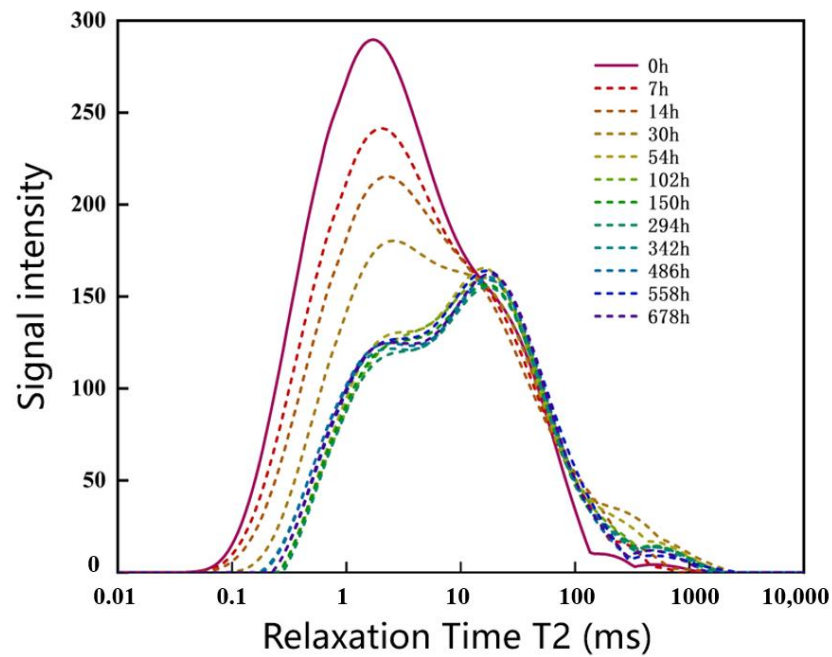
Before experiment

After experiment

(b)

Figure 5. Development of T_2 of sample LYQ at 1 atm. (a) The development of T_2 with time; (b) The new fracture on the surface of the sample after the experiments.

As for the sample LBE, both the porosity (2.7%) and the permeability (1.1×10^{-3} mD, the smallest in all the samples) are small (Figure 6a). This indicates that the pore radii are small. Therefore, the displacement happens first in the small pores. From the development of T_2 over time, it can be seen that micro fractures form in the range of $T_2 = 500\text{--}1000$. The space of new formed micro fractures increases quickly during the first 54 h and then decreases. The new formed micro fractures can also be clearly observed on the surface of the sample after the experiment (Figure 6b). The oil is displaced into large pores with the occurrence of micro fractures due to the swelling of clay mineral after absorption of water. Some oil is retained in the large pores. The displacement efficiency is high, though the pore radii are small. The reason may be that the pore structure/connectivity is good and the capillary is strong (the median value of capillary force is 50 MPa). The high capillary force is also the reason for the large imbibition speed.



(a)



Before experiment

After experiment

(b)

Figure 6. Development of T_2 of sample LBE at 1 atm. (a) The development of T_2 over time; (b) The new fracture on the surface of the sample after the experiments.

Though the initial content of oil and the distribution range of the sample XBL are relatively large, the development speed of imbibition and the displacement efficiency are both very small. One reason may be the low content of IS, and the other that there is no new micro fracture forming. There are two peaks of the initial content of oil in the sample XBL. The first peak is around 1 nm, the smallest in all the samples, so the T_2 spectral that imbibition mainly occurs is the smallest in all samples, which can cause poor connectivity (Figure 7). The very high content of IS and poor connectivity limit the displacement efficiency.

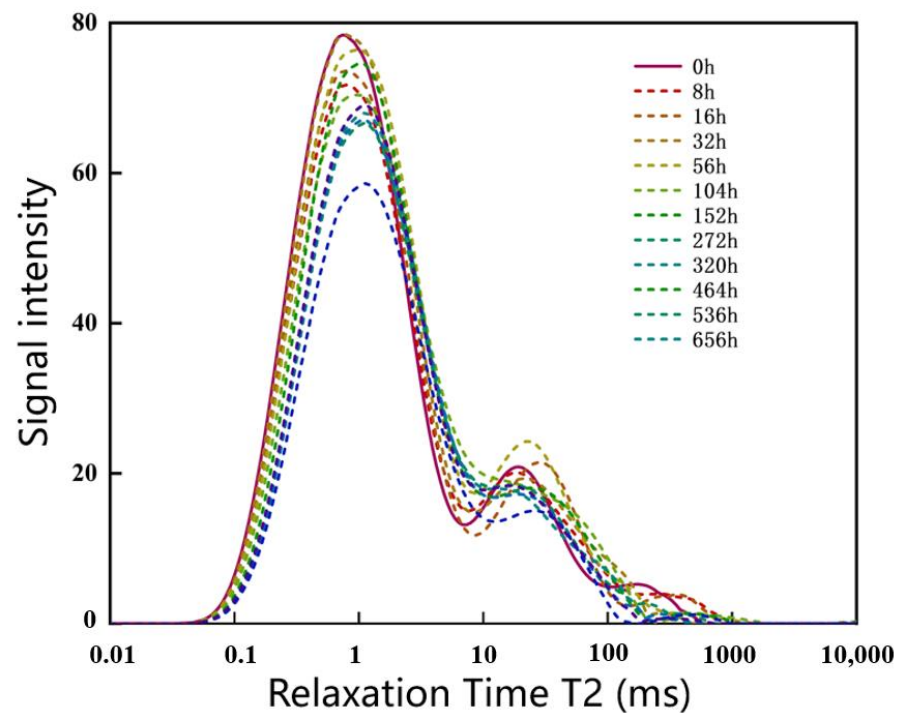


Figure 7. Development of T_2 of sample XBL at 1 atm.

Figure 8 shows the development of T_2 in the sample XEW at 1 atm. The oil is displaced slowly from small pores into large pores. The displacement efficiency is low. The imbibition mass is less. The smallest content of IS in all the samples and high content of quartz causes the low absorption of water and no new micro fractures form. The low displacement efficiency indicates the poor connection of the pore network. Imbibition in a pore network is not only determined by the capillary, viscosity and scale, but also affected greatly by the connection among pores. Poor connection not only increases the complexity of the imbibition path, but also limits the entrance of water into some pores. Subsequently, the imbibition speed and displacement efficiency decrease significantly.

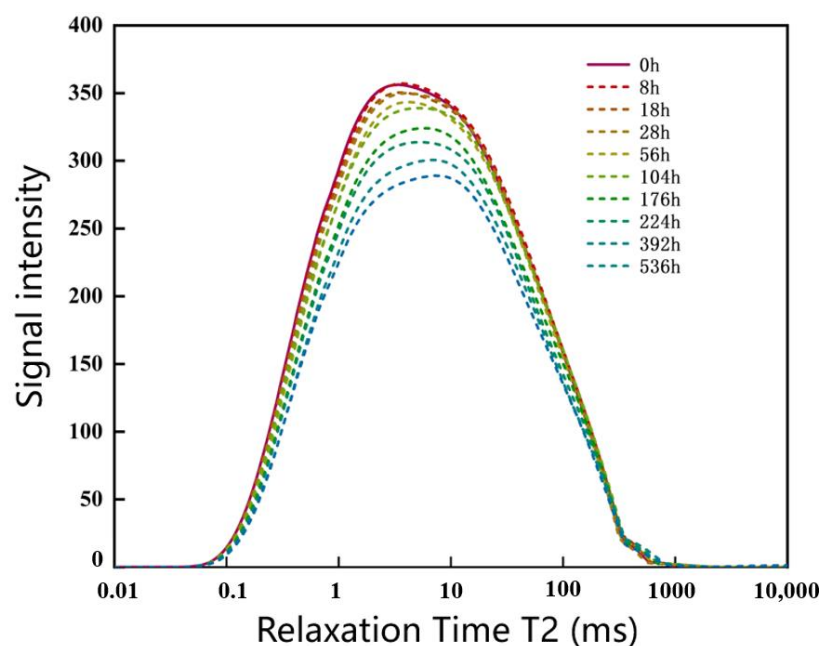


Figure 8. Development of T_2 of sample XEW at 1 atm.

From the above data, it can be seen that the clay minerals in the imbibition in shale rocks are complicated. The comprehensive effects of clay minerals on the imbibition are determined by the combined action of absorption of water and pore structure change due to swelling. When the content of clay minerals is low, the swelling due to absorption of water is weak, and so the effects on the change of pore structure is small, which results in the water mass increase by absorption being larger than the decreased water mass due to pore decrease. Therefore, the imbibition mass increases with the rising of the content of clay minerals. However, the increased mass due to the changes of pore scale and pore structure will overcome the increased mass, due to absorption, when the content of clay minerals is over a designated value. IS has stronger absorption power than the other components in the clay minerals, so its content has more marked effects on the displacement efficiency. The increased imbibition mass does not mean an increase of displacement, because the absorbed water may inter into the intergranular space where there is no oil. In other words, the rapid increase in imbibition mass does not always mean a high displacement of shale rich in clay minerals.

3.2. Comparison of Imbibition under Different Pressures

Under external pressure of 10 MPa, the imbibition of sample XEW develops faster than that under 1 atm and the imbibition mass is larger also (Figure 9). This can be explained by the fact that the median value of capillary force of the sample XEW is 8 MPa, so the pressure gradient increases almost three times that of the pressure of 10 MPa. This indicates that the content of clay minerals is more important to the formation of new micro fractures than pressure. From the development of T_2 , the peaks move toward the right under both pressures. It means the oil in the small pores is displaced into the large pores with imbibition. The sweep area increases faster under 10 MPa than under 1 atm. There are a few new micro fractures which form under 10 MPa (Figure 10). This makes the imbibition faster.

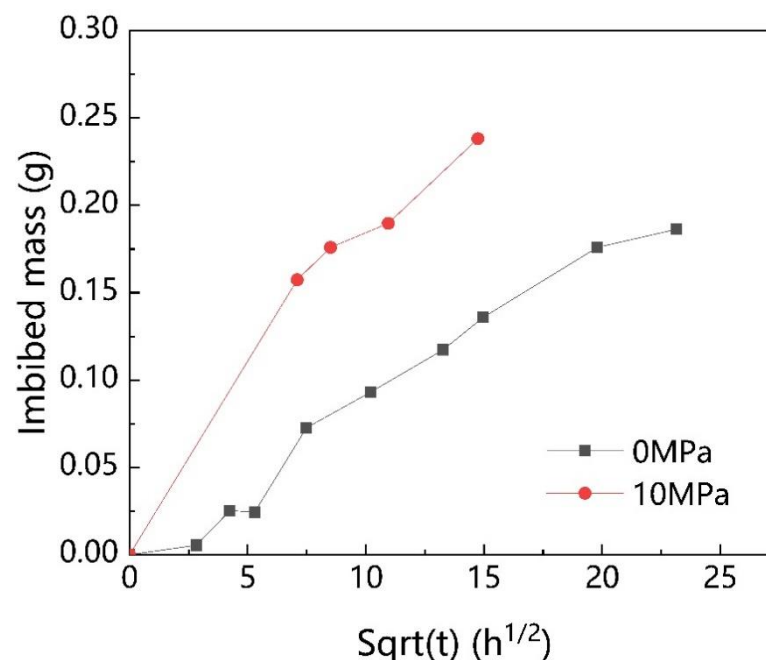
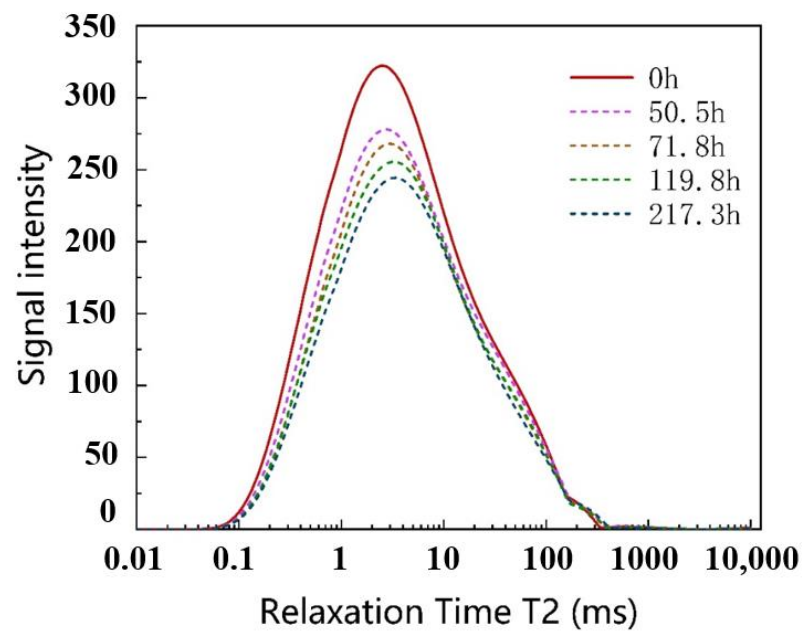


Figure 9. Comparison of imbibition development of sample XEW under 1 atm and 10 MPa, respectively.



(a)



Before experiment

After experiment

(b)

Figure 10. Development of T_2 of sample XEW under 10 MPa. (a) The development of T_2 with time; (b) The new fracture on the surface of the sample after the experiments.

The imbibition speed of the sample XBL under the pressure of 10 MPa is a little larger than that under 1 atm, and the imbibition mass is 12.5% larger than that at 1 atm (Figure 11). Unlike the sample XBL, the imbibition mass under the pressure of 10 MPa is 27% larger than that at 1 atm for the sample XEW (Figure 9). During imbibition under 10 MPa, micro fractures are formed (Figure 12). The reason is that the high content of clay minerals (37.9% for clay minerals and 21.98% for IS) induces large swelling and severe compression of the surrounding pore space. In the meantime, due to the small pore radius and small porosity, the connectivity becomes poor. Therefore, the permeability decreases with the swelling due to the absorption of water. Since a considerable part of the water is sucked into the intergranular space of the clay minerals, the remaining water to displace the oil is less, so the displacement efficiency is low. The oil is more obviously displaced from small pores into large pores under 10 MPa than under 1 atm due to the formation of more micro fractures.

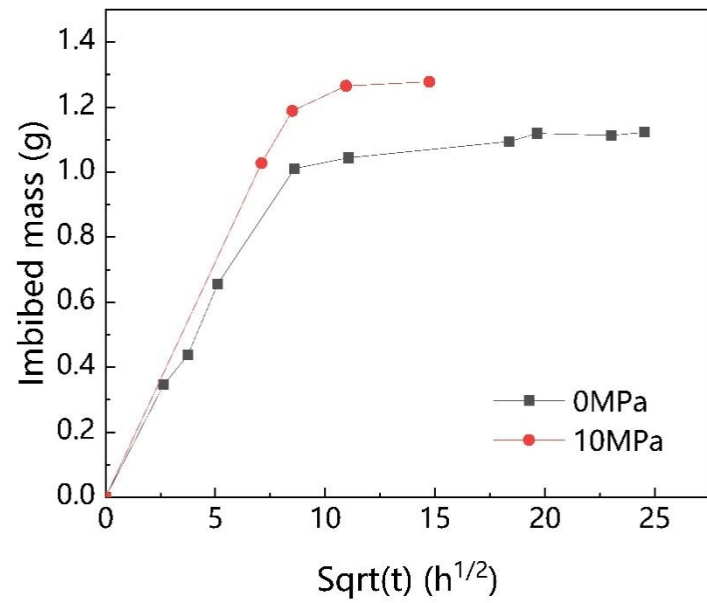
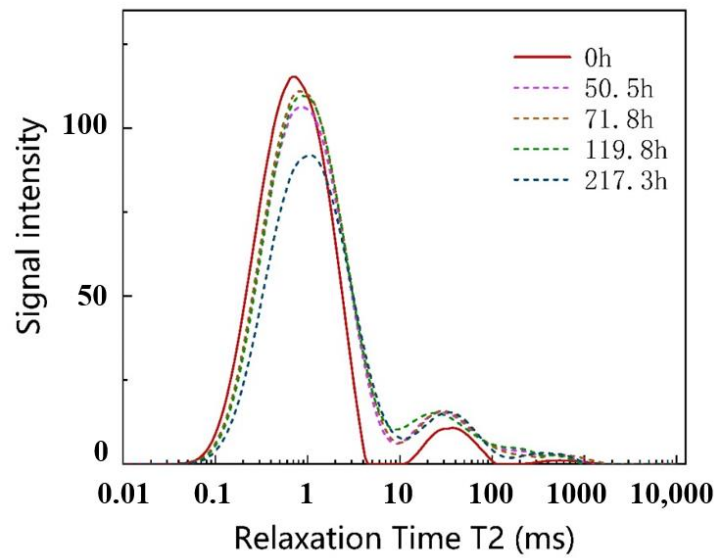
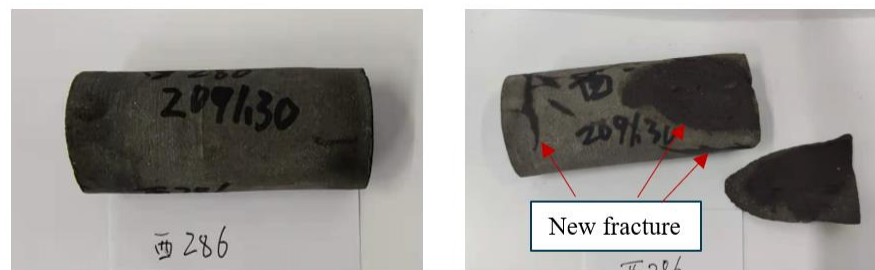


Figure 11. Development of imbibition mass of sample XBL under 1 atm and 10 MPa.



(a)



Before experiment

After experiment

(b)

Figure 12. Development of T_2 of sample XBL under 10 MPa. (a) The development of T_2 with time; (b) The new fracture on the surface of the sample after the experiments.

The effects of external pressure are remarkable on the imbibition of the sample YSS. The imbibition mass under 10 MPa is 26.1% larger than that under 1 atm (Figure 13). The reason may be the large permeability relative to the other samples. In the spontaneous imbibition process of this sample, more water enters the small pores than the large pores (Figure 14). Considering the pressure p , the driving force of the imbibition is $(p + p_c)$. With the increase of pressure, the effects of the capillary become relatively less, especially for the samples with small capillary force. If the capillary force can be neglected when it is much smaller than the pressure, the imbibition speed is determined mainly by the external pressure and the imbibition mass increases with the increase in permeability.

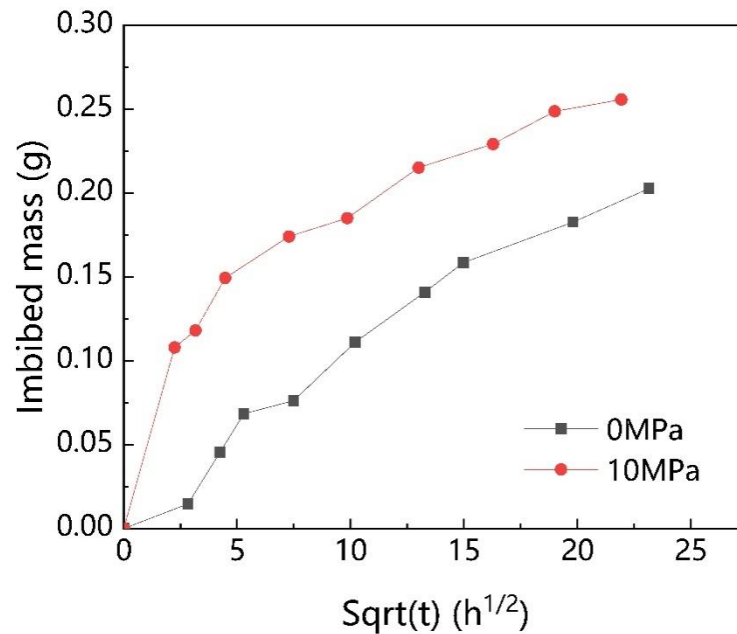


Figure 13. Development of imbibition mass of sample YSS under 1 atm and 10 MPa.

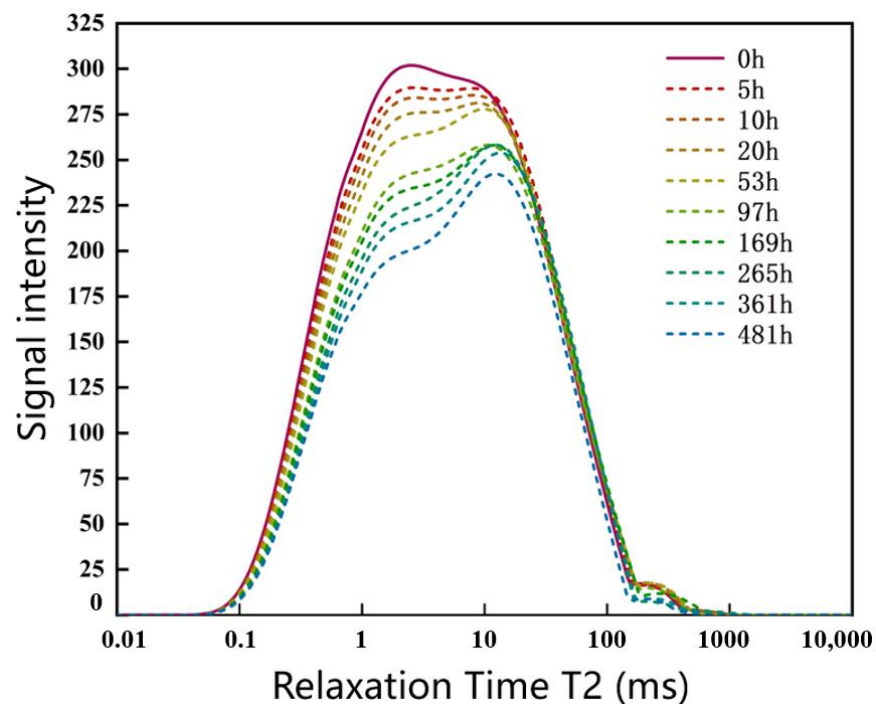


Figure 14. Development of T_2 of sample YSS under 10 MPa.

3.3. The Displacement Efficiency

The displacement efficiency, the mass ratio of displaced oil to the total oil in the same sweep area, is an important factor that concerns engineers very much in practice. Shown in Figures 15–17 are the relations between the displacement efficiency and the contents of the IS, clay minerals, porosity and permeability, respectively. None of these factors with the displacement is in a monotonous relation. It indicates that the relation between these factors and the displacement efficiency is complicated. For example, if the rocks have a close porosity but remarkably different permeability, then the lower the permeability, the larger the capillary force is, and the pores joining in imbibition are more, so the displacement efficiency is higher. The clay minerals can either protect or block up the intergranular pores due to swelling and migration of clay minerals after absorption of water [27].

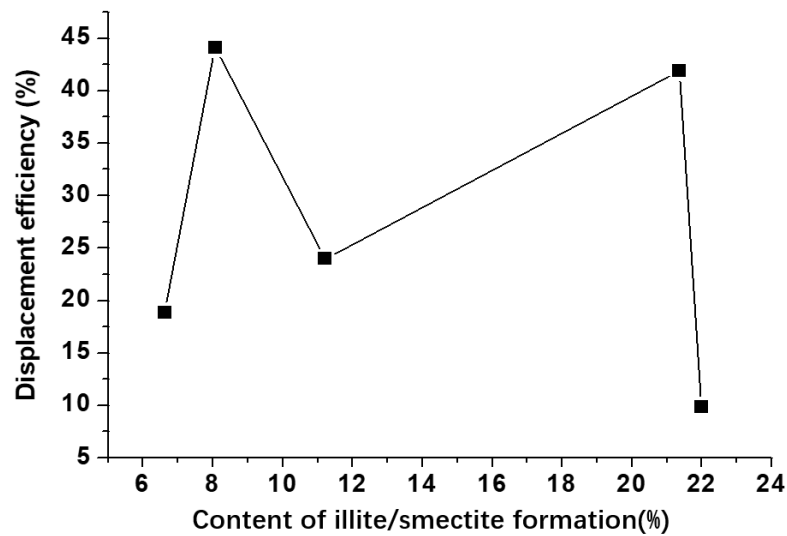


Figure 15. The efficiency of oil displacement under 1 atm versus the content of illite/smectite.

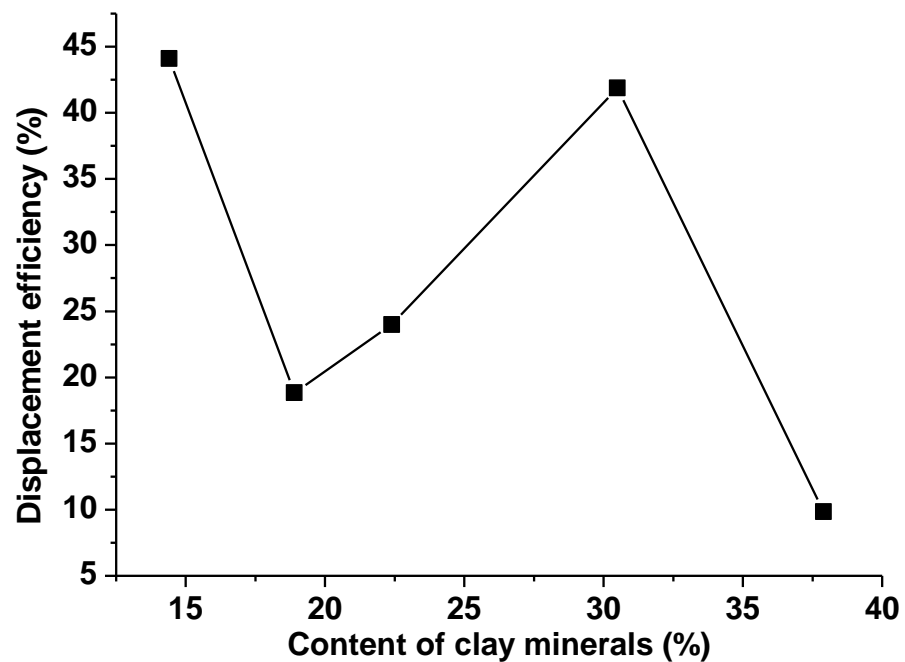


Figure 16. The efficiency of oil displacement under 1 atm versus the content of clay minerals.

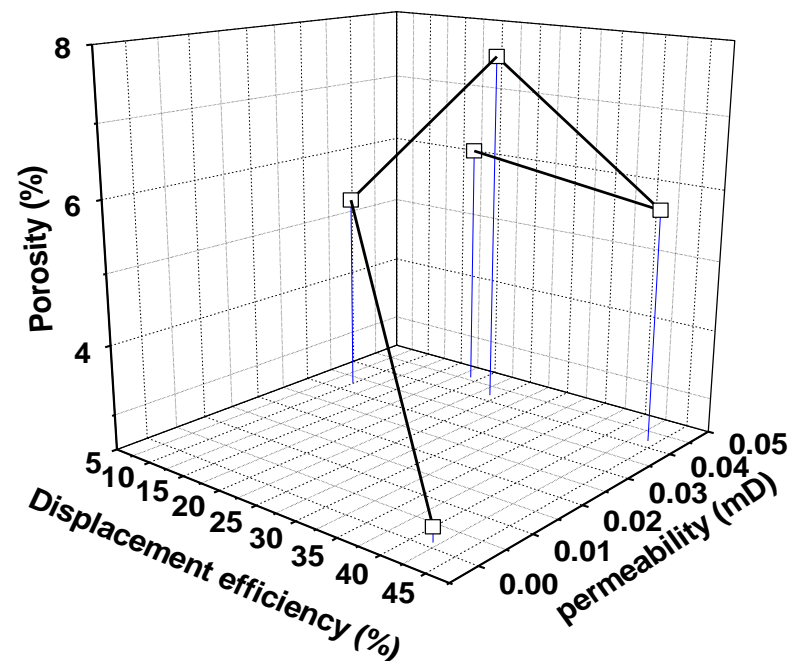


Figure 17. Displacement efficiency versus permeability and porosity.

The characteristics of strong absorption of water causes the shale with high content of IS to swell significantly, then the pore scale shrinks and the pore connection becomes weak, and these changes result in the decrease of sweep area and displacement efficiency. On the other hand, the absorbed water can lead to changes of the wetting conditions of pores and the formation of micro fractures, which can cause increase in efficiency. IS has a stronger power of absorbing water than the other components in the clay minerals, so its content has more marked effects on the displacement efficiency. When the content of IS is low, the swelling due to absorption of water has little effects on the changes of pore structure. However, the swelling may significantly change the wetting conditions and even cause the occurrence of new micro fractures. That means that the content of absorbed water is larger than the content of discharged water due to the compaction of pores. Therefore, the displacement efficiency increases with the rising of the content of IS. When the content of IS rises above some value, the decreased displacement efficiency due to the changes of pore scale and structure will overcome that due to absorption of water. Many new micro fractures will form when the content of IS increases; furthermore, the displacement efficiency can increase again (Figures 15 and 16). Therefore, the effects of IS on the displacement efficiency are multiple. The practical results of IS on the displacement are the comprehensive effects of these factors.

Porosity and permeability characterize the development degree, uniformity and the connectivity of the pores in a shale. The porosity creates the potentially largest space for storage of fluid. The permeability is responsible for the seepage power. Unlike conventional rock, the porosity and the permeability are not directly related with each other in the shale because of the complex distribution and structure of pore/fracture network. So both these two factors affect the displacement efficiency significantly.

Noting that the other factors are not constants when we discuss the relation between the displacement and one of the minor factors, the characteristics above show the comprehensive effects of all the factors. For example, we consider the relation between the displacement efficiency and two main factors: the content of IS and the radius. To draw the curve of these three factors in a three-dimensional coordinate, it can be seen that the curve is neither monotonous nor smooth, which indicates that these two factors alone cannot determine the displacement efficiency (Figure 17).

In total, the displacement mechanism of the shale is the comprehensive effect of many factors. In practice, quantitative relation between the displacement efficiency and the main factors should be studied and presented further.

4. Discussion

Presence of clay minerals is one of the main challenges in the exploitation of shale reserves. Water adsorption by clay minerals can not only cause swelling, but also damage the permeability of rock. Swelling of clay minerals is thought to be one of the main reasons for the formation of new micro fractures [28,29]. Meng et al. [14] found by experiment that the swelling of clay minerals causes not only organic but also inorganic cracks. The permeability increases with organic cracks. They observed new formed micro fractures by NMR and scanning electron microscopy. They found that large T_2 (information measured by NMR) occurs with the formation of micro fractures during imbibition. The phenomenon of micro fracture formation during imbibition in this literature is similar to the results of our experiments. Besides micro fractures and macro fractures can form, and even damage the samples in some cases.

In fact, the initiation and development of new micro fractures in shale is determined by the interaction between the water and the clay minerals. When the shale adsorbs water, hydration will occur on the crystal layer of the clay minerals. Swelling happens with the increase of the repulsion between crystals. Meanwhile, the adsorbed water causes the threshold stress of the fractures. These two factors improve the initiation and development of fractures in shale. Once new fractures form, permeability will clearly increase because the fractures have stronger filtration power and have the function to enhance the connection among pores.

To understand the initiation of micro fractures due to adsorption of water in shale containing clay minerals, it is important to observe the structural changes of mineral crystals and pores over time. Therefore, more microscopic observation with CT, scanning electron microscopy etc. is necessary in the future experimental study.

5. Conclusions

To investigate the effects of clay minerals and external pressures on the imbibition of shales, experiments were processed and the development of imbibition mass and the T_2 spectral with time were measured and analyzed. The main conclusions are as follows.

The low content of illite and IS and small capillary force lead to small imbibition mass and speed. New fractures formed during imbibition can increase permeability. Accordingly, the imbibition will be speeded up. The pore structure, the content of illite and IS and capillary force significantly affect the imbibition process.

The external pressure obviously affects the imbibition speed and the final imbibition mass. The content of clay minerals is more important for the formation of new micro fractures than the pressure. The effects of pressure on the imbibition are related with the capillary force, pore structure, formation and new micro fracture, etc.

The displacement mechanism of shale is the comprehensive effect of many factors. The relation between main factors and the displacement efficiency is complicated. Quantitative relations between the displacement efficiency and the main factors should be studied further and developed.

Author Contributions: Conceptualization, Y.L.; methodology, X.Z.; software, L.L.; validation, J.L.; resources, J.L.; data curation, L.L.; writing—original draft preparation, L.L.; writing—review and editing, L.L. and Y.L.; visualization, L.L.; supervision, Y.L. and J.L.; project administration, F.M.; All authors have read and agreed to the published version of the manuscript.

Funding: This research received no external funding.

Conflicts of Interest: The authors declare no conflict of interest.

References

1. Guo, J.; Li, M.; Chen, C.; Tao, L.; Liu, Z.; Zhou, D. Experimental investigation of spontaneous imbibition in tight sandstone reservoirs. *J. Pet. Sci. Eng.* **2020**, *193*, 107395. [[CrossRef](#)]
2. Shen, Y.; Ge, H.; Zhang, X.; Chang, L.; Liu, D.; Liu, J. Impact of fracturing liquid absorption on the production and water-block unlocking for shale gas reservoir. *Adv. Geo-Energy Res.* **2018**, *2*, 163–172. [[CrossRef](#)]
3. Makhanov, K.; Habibi, A.; Dehghanpour, H.; Kuru, E. Liquid uptake of gas shales: A workflow to estimate water loss during shut-in periods after fracturing operations. *J. Unconv. Oil Gas Resour.* **2014**, *7*, 22–32. [[CrossRef](#)]
4. Yang, L.; Ge, H.; Shi, X.; Cheng, Y.; Zhang, K.; Chen, H.; Shen, Y.; Zhang, J.; Qu, X. The effect of microstructure and rock mineralogy on water imbibition characteristics in tight reservoirs. *J. Nat. Gas Sci. Eng.* **2016**, *34*, 1461–1471. [[CrossRef](#)]
5. Li, C.; Singh, H.; Cai, J. Spontaneous imbibition in shale: A review of recent advances. *Capillarity* **2019**, *2*, 17–32. [[CrossRef](#)]
6. Cai, J.; Li, C.; Song, K.; Zou, S.; Yang, Z.; Shen, Y.; Meng, Q.; Liu, Y. The influence of salinity and mineral components on spontaneous imbibition in tight sandstone. *Fuel* **2020**, *269*, 117087. [[CrossRef](#)]
7. Yildiz, H.O.; Gokmen, M.; Cesur, Y. Effect of shape factor, characteristic length, and boundary conditions on spontaneous imbibition. *J. Pet. Sci. Eng.* **2006**, *53*, 158–170. [[CrossRef](#)]
8. Feng, Q.; Xu, S.; Xing, X.; Zhang, W.; Wang, S. Advances and challenges in shale oil development: A critical review. *Adv. Geo-Energy Res.* **2020**, *4*, 406–418. [[CrossRef](#)]
9. Makhanov, K.; Dehghanpour, H.; Kuru, E. An Experimental Study of Spontaneous Imbibition in Horn River Shales. In Proceedings of the SPE Canadian Unconventional Resources Conference, Calgary, AB, Canada, 30 October–1 November 2012.
10. Meng, M.; Ge, H.; Ji, W.; Shen, Y.; Su, S. Monitor the process of shale spontaneous imbibition in co-current and counter-current displacing gas by using low field nuclear magnetic resonance method. *J. Nat. Gas Sci. Eng.* **2015**, *27*, 336–345. [[CrossRef](#)]
11. Morsy, S.; Sheng, J.J. Imbibition Characteristics of the Barnett Shale Formation. In Proceedings of the SPE Unconventional Resources Conference, The Woodlands, TX, USA, 1–3 April 2014.
12. Wang, Z.; Li, X.; Wei, Y.; Qin, L.; Lu, H. NMR technologies for evaluating oil & gas shale: A review. *Chin. J. Magn. Reson.* **2015**, *32*, 688–698.
13. Gupta, A.; Xu, M.; Dehghanpour, H.; Bearinger, D. Experimental Investigation for Microscale Stimulation of Shales by Water Imbibition during the Shut-in Periods. In Proceedings of the SPE Unconventional Resources Conference, Calgary, AB, Canada, 15–16 February 2017.
14. Meng, M.; Ge, H.; Shen, Y.; Li, L.; Tian, T.; Chao, J. The effect of clay-swelling induced cracks on shale permeability during liquid imbibition and diffusion. *J. Nat. Gas Sci. Eng.* **2020**, *83*, 103514. [[CrossRef](#)]
15. Zheng, X.; Liu, J.; Bian, K.; Liu, S.-G.; Liu, Z.; Ai, F. Softening micro-mechanism and mechanical properties of water-saturated shale in Northwestern Hubei. *Rock Soil Mech.* **2017**, *38*, 2022–2028.
16. Ling, S.X.; Wu, X.Y.; Sun, C.W.; Liao, X.; Ren, Y.; Li, X.N. Experimental study of chemical damage and mechanical deterioration of black shale due to water-rock chemical action. *J. Exp. Mech.* **2016**, *31*, 511–524.
17. Bonnelye, A.; Schubnel, A.; David, C.; Henry, P.; Guglielmi, Y.; Gout, C.; Fauchille, A.; Dick, P. Strength anisotropy of shales deformed under uppermost crustal conditions. *J. Geophys. Res. Solid Earth* **2017**, *122*, 110–129. [[CrossRef](#)]
18. Hu, M.M.; Hueckel, T. Environmentally enhanced crack propagation in a chemically degrading isotropic shale. In Proceedings of the Bio-and Chemo-Mechanical Processes in Geotechnical Engineering: Géotechnique Symposium in Print 2013, London, UK, 3 June 2013; ICE Publishing: London, UK, 2013.
19. Zhang, J.; Chenevert, M.E.; AL-Bazali, T.; Sharma, M.M. A New Gravimetric-Swelling Test for Evaluating Water and Ion Uptake in Shales. In Proceedings of the SPE Annual Technical Conference and Exhibition, Houston, TX, USA, 26–29 September 2004.
20. Li, J.; Li, X.; Wang, X.; Li, Y.; Wu, K.; Shi, J.; Yang, L.; Feng, D.; Zhang, T.; Yu, P. Water distribution characteristic and effect on methane adsorption capacity in shale clay. *Int. J. Coal Geol.* **2016**, *159*, 135–154. [[CrossRef](#)]
21. Zhang, Y.; Ge, H.; Shen, Y.; Jia, L.; Wang, J. Evaluating the potential for oil recovery by imbibition and time-delay effect in tight reservoirs during shut-in. *J. Pet. Sci. Eng.* **2020**, *184*, 106557. [[CrossRef](#)]
22. Yang, Y.; Li, Y.; Yao, J.; Zhang, K.; Iglauer, S.; Luquot, L.; Wang, Z. Formation damage evaluation of a sandstone reservoir via pore-scale X-ray computed tomography analysis. *J. Pet. Sci. Eng.* **2019**, *183*, 106356. [[CrossRef](#)]
23. Mattax, C.C.; KYTE, J.R. Imbibition oil recovery from fractured, water-drive reservoir. *Soc. Pet. Eng. J.* **1962**, *2*, 177–184. [[CrossRef](#)]
24. Kazemi, H.; Gilman, J.R.; Elsharkawy, A.M. Analytical and numerical solution of oil recovery from fractured reservoirs with empirical transfer functions. *SPE Reserv. Eng.* **1992**, *7*, 219–227. [[CrossRef](#)]
25. Shouxiang, M.; Morrow, N.R.; Zhang, X. Generalized scaling of spontaneous imbibition data for strongly water-wet systems. *J. Pet. Sci. Eng.* **1997**, *18*, 165–178. [[CrossRef](#)]
26. Yang, L.; Dou, N.; Lu, X.; Zhang, X.; Chen, X.; Gao, J.; Yang, C.; Wang, Y. Advances in understanding imbibition characteristics of shale using an NMR technique: A comparative study of marine and continental shale. *J. Geophys. Eng.* **2018**, *15*, 1363–1375. [[CrossRef](#)]
27. He, M. Research on Imbibition Mechanism of Tight Sandstone Reservoir. Ph.D. Thesis, Yangtze University, Jingzhou, China, 2017.
28. Chenevert, M.E. Shale alternation by water adsorption. *J. Petrol. Tech.* **1970**, *22*, 1141–1148. [[CrossRef](#)]
29. Sun, L.; Tuo, J.; Zhang, M.; Wu, C.; Wang, Z.; Zheng, Y. Formation and development of the pore structure in Chang 7 member oil-shale from Ordos Basin during organic matter evolution induced by hydrous pyrolysis. *Fuel* **2015**, *158*, 549–557. [[CrossRef](#)]